J. Agr. Sci. Tech. (2021) Vol. 23(1): 107-123

Canopy Based Aboveground Biomass and Carbon Stock Estimation of Wild Pistachio Trees in Arid Woodlands Using GeoEye-1 Images

R. Bagheri[1], S. Shataee Jouibary[1*], and Y. Erfanifard[2]

ABSTRACT

Spatially explicit estimates of aboveground biomass over large area are necessary for natural resources managers. This study examined aboveground biomass and carbon stock of the wild pistachio (*Pistacia atlantica*) based on individual tree crown detection and allometric development in the arid woodlands using high-resolution satellite images of GeoEye-1 in a reserved forest area of Wild Pistachio trees in the South Khorasan Province, East of Iran. Biomass of sampled trees was determined using field sampling and experimental tests. In addition, the biomass of stems was determined using volume and density. The allometric biomass and carbon stock equations of Wild Pistachio trees were developed based on crown area, diameter at breast height (1.3 m), and height of trees. The trees crowns were detected and delineated on the GeoEye-1 images, using local maxima filters, and region growing segmentation algorithms, respectively. In addition, a morphological watershed transformation method was applied to split the connected and overlapped tree crowns. Performing algorithms was assessed using the measured field crown of sample trees by precision, recall, and overall accuracy indices. The biomass and carbon stock of trees of the study area were estimated using delineated crown area and the developed allometric equations. The results showed that the equation that used crown area could explain more than 80% of the remarked variation in biomass and carbon stock. In addition, the crown detection method results showed that overall detection rate and the quality of crown boundaries were acceptable. In conclusion, the study confirmed that combining the allometric equations with crown information from high-resolution images could contribute to the explicit mapping of biomass and carbon stock of wild pistachio trees in the arid woodlands.

Keywords: Allometric equations, Object-based, *Pistacia atlantica*, Tree crown delineation.

INTRODUCTION

The wild pistachio (*Pistacia atlantica*), as a deciduous-broadleaved species, is dominant at this vegetation zone as one of the ecologically most important and native species of Iran. The wild pistachio forest stands play an important role in preventing destructive floods and helping soil conservation in the arid and semi-arid regions (Lal, 2004). Drylands are considered to have great potential for carbon sequestration and, therefore, could play an important role in combating the global climate change (FAO, 2004). Woodlands in the arid and semi-arid regions are facing desertification or degradation caused by human and climate change. The carbon kept in the aboveground living biomass of trees is typically the largest pool and directly affected by deforestation and degradation

[1] Department of Forestry, Gorgan University of Agricultural Science and Natural Resources, Gorgan, Islamic Republic of Iran.
[2] Department of Remote Sensing and GIS, Faculty of Geography, University of Tehran, Tehran, Islamic Republic of Iran.
*Corresponding author; e-mail: Shataee@gau.ac.ir

[DOR: 20.1001.1.16807073.2021.23.1.6.9]

(Gibbs *et al.,* 2007). The international debate on Reducing Emissions of greenhouse gases from Deforestation and forest Degradation (REDD) has called for rigorous carbon stock measuring, reporting and corroborating the methods (Mukono and Sambaiga, 2016). Aboveground Biomass (hereafter, AGB) includes between 70 and 90% of total forests biomass (Cairns *et al.,* 1997).

Accurate measurement of the tree biomasses and carbon stocks and their temporal and spatial variations in the woodlands are important for the use and protection of woodland resources. Although the biomass data gathered from field data measurements is the most accurate, it is not a practical approach for broad-scale assessments since it is destructive. Different remote-sensing data sources and techniques have emerged as promising alternatives, particularly with collecting high-resolution imagery, allowing for individual-tree-level measurements such as height and crown area (Drake *et al.,* 2003). So far, the researchers have tried to estimate the aboveground biomass by medium (Li *et al.,* 2019; Wu *et al.,* 2016; Mousavi, 2015) to high spatial resolution (Eckert, 2012; Hussin *et al.,* 2014) satellite data. The medium and coarse spatial resolution imageries have always been a potential AGB estimator at the national and regional scale, but in the sites with a complex biophysical environment, it possesses problems like mixed pixel and data saturation (Goetz *et al.,* 2009). However, for plot level estimates of high-precision results, especially for extracting the canopy crown, applying the high spatial resolution data is necessary. The high spatial resolution imagery has proper capacity for finer detection and recognition of spectral reflections of tree crowns and having lower mixed pixels in the edge of crowns. There are many pixel-based and object-based methods to detect and delineate the canopy crown on the 2D and colour-based optical imageries as well as 3D Lidar (Light Detection and Ranging) or photogrammetric point clouds data. Using proper techniques for accurate delineation and extraction of tree crown area as a segment or object is very important at tree level or individual tree-based estimates on high-resolution images. The most popular methods for automatic individual tree crown segmentation described in the literature are detecting local maxima, region growing techniques, edge detection, and watershed segmentation (Saliola, 2014). The benefit of region growing and watershed segmentation, which also is implemented on object-based software such as eCognition, is that they can both be used to analyze high spatial resolution images.

The object-based approaches do not run directly on individual pixels, but rather on objects consisting of many pixels that are grouping together in a meaningful way by image partition. This approach, when undertaken with geospatial data, are often termed as Geographic Object-Based Image Analysis (GEOBIA) (Hay and Castilla, 2008). Commercial software, such as the eCognition package (Definiens, 2006), provides the object-based classifiers, but they are supervised and need human intervention. Several automated and semi-automated approaches have been developed to extract objects from satellite data, especially for high spatial resolution data (Benediktsson *et al.,* 2003; Evans *et al.,* 2002; Huang and Zhang, 2008; Mayer, 2008; Myint *et al.,* 2011). Remote sensing and Geographic Information System (GIS) are some of the indirect approaches that can adequately avoid the challenges associated with conventional biomass estimation methods (Brown, 2002); making it possible to measure and survey biomass in large areas with potentially low cost and less time (Wulder *et al.*, 2008; Drake *et al.*, 2002).

The relationship between stem Diameter at Breast Height (DBH) and Crown Projection Area (CPA) of a tree enables calculation of AGB (Feldpausch *et al.,* 2011). Recent developments in high resolution space-borne and airborne remote sensing data have provided an opportunity to better estimate and map AGB across different spatial and temporal scales. Challenges with using the

[DOR: 20.1001.1.16807073.2021.23.1.6.9]

crown area as a predictor variable still remain, ranging from inability to measure crown area accurately to lack of consistent allometric equations (Gibbs *et al.,* 2007). Kuyah *et al*. (2012) studied crown area variable for estimation of aboveground tree biomass in agricultural landscapes of western Kenya and the results showed that the equations developed to fit the data well with about 85% of the observed variation in AGB explained by crown area. The object-based image analysis is providing new opportunities to improve biomass and carbon stock estimation and mapping by delineating and classifying a crown projection area of individual trees. Many researchers (Brandtberg and Walter, 1998; Leckie *et al.,* 2003; Erikson and Olofsson, 2005; Ke and Quackenbush, 2011; Pu and Landry, 2012) could study individual tree crown delineation or segmentation using high-resolution images. Tree crown delineation and extraction are important to obtain information at the individual tree level. Several algorithms have been presented for automatic individual tree delineation and crown extraction on satellite images, such as region growing, watershed segmentation, and template-matching-based methods (Ke and Quackenbush 2011). The region growing approach assumes that the center of a crown is brighter than the edge of the crown (Culvenor, 2002). Thus, detecting the brightest pixel of the crown gives a chance to find the crown center, and growing a region from the crown center based on illumination image helps to delineate tree crowns (Ke and Quackenbush, 2007). Culvenor (2002) applied a region-growing approach from local maxima and resulted in up to 77% of agreement between segmented tree crowns and digitized tree crowns. Zaki *et al.* (2015) studied an individual tree crown delineation method for tropical lowland Dipterocarp using watershed transformation algorithm. Their results showed the watershed transformation algorithm was suitable to delineate the tree crown of the tropical lowland Dipterocarp forest area. Therefore, it is given that performance of algorithms for crown delineating can be different based on tree and in any studies. Therefore, its ability should be investigated based on the shape of crowns, canopy cover conditions, and satellite images.

The first objective of this study was to introduce a tree crown delineation method on the GeoEye imagery for Wild Pistachio trees crown extraction in the sparse woodlands. The other objective was to create and find the proper allometric equation based on extracted tree crowns to estimate the AGB and carbon stocks through a nondestructive method for Wild Pistachio trees in the center and east of Iran.

MATERIALS AND METHODS

Study Area

The Irano-Touranian vegetation zone is extensive and covers the center and east of Iran. It is one of the five different vegetation zones in Iran having an arid and semi-arid climate, with an area of 3.5 million hectares. The study was carried out in Tage-e Ahmad Shahi, which is a reserve forest of wild pistachio trees and covers an area of 25 km^2, however, the core zone of reserve forest with 5.15 km2 area (red doted line) was selected for this study. (Figure 1). This region is located in Nehbandan County, South Khorasan Province of Iran, and lies between 60° 10' E to 60° 16' E longitudes and 31° 53' N to 31° 57' N latitudes. The average annual rainfall is about 180 mm, the climate is typically arid (average annual temperature of 21.2^{o}C, maximum of 45^{o}C), with hot and intensive radiation in the summer, and the mean of altitude is 1,800 m above the sea level. The reserved area includes a pure stand of *Pistachio Atlantica;* but a few other associated shrubs such as *Pteropyrum aucheri*, *Atraphaxis spinosa* and *Ephedra strobilacea* and some bushes such as *Achillea wilhelmsii* and *Astragalus schistocalyx* are seen in the study area.

[DOR: 20.1001.1.16807073.2021.23.1.6.9]

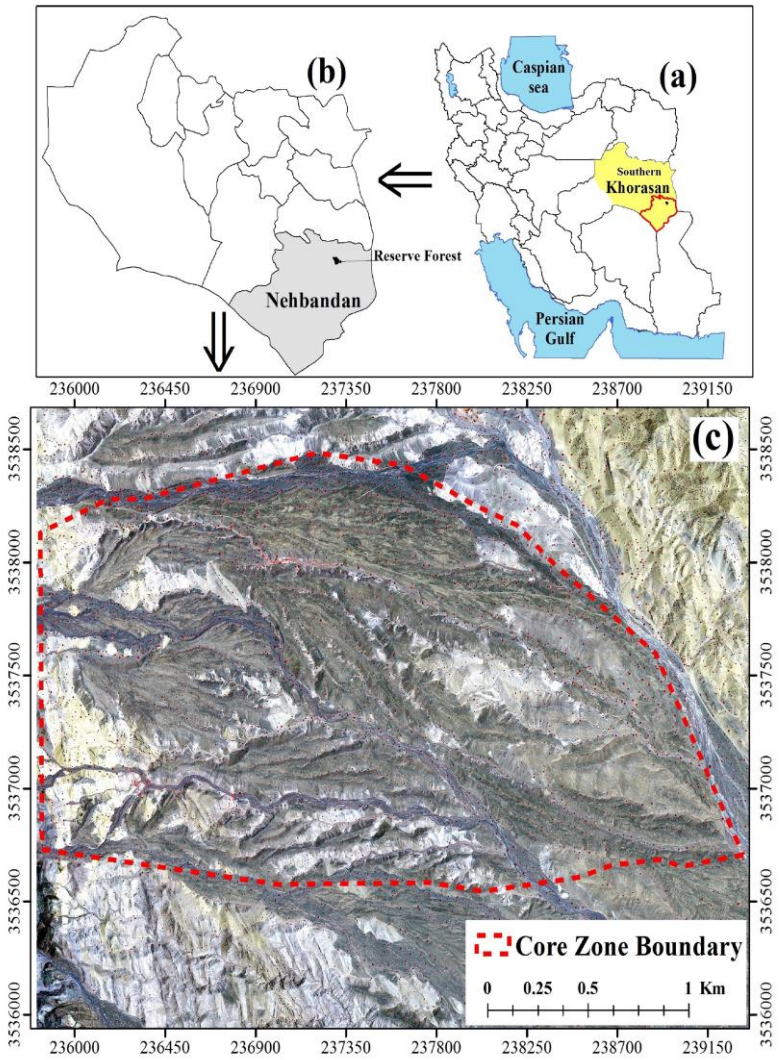

Figure 1. (a) Location of study area in Iran; (b) southern Khorasan Province; and (c) The boundary of the study area overlaid with a false color composite (432) of Geo-Eye1 image.

Datasets

In this study, we used the GeoEye-1 VHRS images, with a spatial resolution of panchromatic and multispectral 0.5 and 2 m, respectively, which was acquired on 30 August 2012. The GeoEye-1 multispectral image consists of four spectral bands in the visible and NIR part of the electromagnetic spectrum, including blue (450–510 nm), green (510–580 nm), red (655–690 nm), near-infrared (780– 920 nm), and panchromatic (450–800 nm).

About 145 wild pistachio trees, which had different canopy area sizes with 2.5 to 89.3 m^2, were selected for field sampling. The biophysical attributes including crown area, DBH, and crown diameter; and tree heights were measured accurately by different tools. The tree crown ground truth was prepared through accurate positioning of trees by Trimble DGPS using Post Processing Kinematic (PPK) method and surveying the boundary points of crowns by Total Station surveying instrument (Figure 3). In addition, the positions of all trees in 60 plots (1-hectare area) were registered using Trimble R3 DGPS

[DOR: 20.1001.1.16807073.2021.23.1.6.9]

by the Post Processing Kinematic (PPK) method. These positions were used for accuracy assessment of the tree detection and delineations. From the previous stage on sample trees (145 trees), 30 trees with different diameters and crown sizes were randomly selected and their quantitative variables were measured for biomass and carbon stock estimation. Considering the legal rules limitation and prohibition of the tree cutting and foliage falling in the reserved area, generally, the biomass measurement of tree trunks is calculated using the volume and wood density of tree species. In this study, the calculated volume from field measuring the DBH and height of trees and wood density of pistachio trees from laboratory measuring were used for trunk biomass estimations. For stem density calculation, a selected tree was cut and then, some samples from different sections of the stem were sampled and wet weights of samples were measured using a balance. In addition, the crown biomass of trees including foliage and thin stems was determined using a subsampling method. In this method, a quarter of leaves, stems, and branches from the 30 sample trees were selected and cut and then the wet weights of 30 leaves, stems, and branches with different diameters and sizes were selected and weighed immediately. The samples were transported to the laboratory to measure the dry weight, wood density, and carbon stock. The samples were oven-dried at 75 ^{o}C (24 h) and weighed after weight stabilization. The Biomass of each Component (BC) including leaves, branches, and stems was determined as a product of the Fresh (wet) Weight of parts (FWc) and the ratio of 'Dry Weight (DWs): Fresh Weight (FWs)'of the sample was computed as Equation (1). Enough quantity of each component was burned in electric Kiln to calculate the carbon stock.

$$B_c = \frac{FW_c \times DW_s}{FW_s} \quad (1)$$

The satellite images were ortho-rectified using rational polynomial coefficients and a horizontal 20-m topographic digital elevation model in Universal Transverse Mercator (UTM) coordinate system and the WGS84 datum. A Differential Global Positioning System (DGPS) receiver was used for the accurate assessment of ortho-rectified satellite dataset. The permanent reference point was acquired from the National Cartographic Center of Iran (NCC), to fix the reference DGPS set at that particular point. The HPF fusion algorithm (Chavez *et al.*, 1991) was used to merge the panchromatic and multispectral images for producing the pan-sharpened four-band images with 0.5 m resolution and similar spectral characteristics (Figure 2). The GEOBIA methodology was implemented on the Digital Values (DNs) of the pan-sharpened images. Before segmentation, a low pass median filter (3 by 3 kernel size) on fused images was applied to avoid over-segmentation (Platt and Schoennagel, 2009) to produce more homogeneous image segments. Applying low pass median filter reduced the number of convolutions in the final segmented polygons because of the VHRS images (Mora *et al.*, 2010). A Normalized Difference Vegetation Index (NDVI) data was created from the GeoEye-1 images for applying local maxima filtering as a start point of region growing segmentation performance.

Allometric Equation Development

To estimate biomass and carbon stock of delineated trees from the satellite image, the relationship between the biophysical features (i.e. DBH, tree and crown heights and crown area) and the biomass and carbon stock of all sampled trees were developed for this species. Several empirical methods were available for biomass and carbon stock estimation. However, in this study, we preferred using allometric equations because an allometric model is a useful tool that can estimate the biomass and carbon stock of single trees according to some easily measured variables by satellite images, such as crown area (Brown, 1997). Allometric equations between lab-calculated rates of biomass and carbon stocks and tree feature, particularly crown area and crown

[DOR: 20.1001.1.16807073.2021.23.1.6.9]

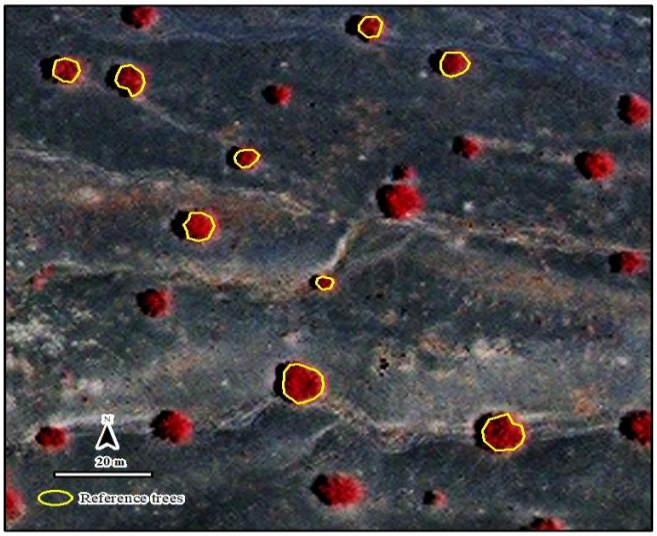

Figure 2. Tree crown reference polygons of the sample trees on a Pan-sharpened false colour composite of GeoEye-1images.

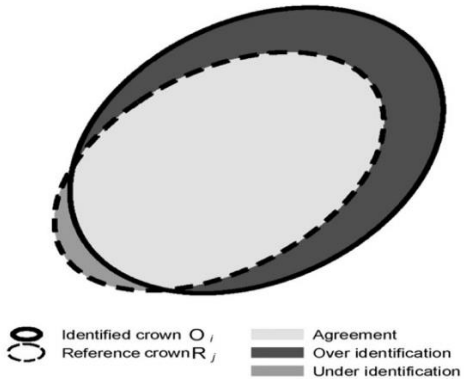

Figure 3. Over-identification and under-identification for a reference object R_j and an identified object O_i (Ardila *et al.*, 2012).

diameters, were investigated using different regression models. The most common regression allometric model in biomass studies is the power function (Brown, 1997) as Equation (2), which was developed by Sohrabi and Shirvani (2012) for estimating standing biomass of *Pistachio Atlantica* with a power regression model. We used this model for allometric equations, too.

$$Y = b_0 x^{b_1} \quad (2)$$

Where, Y is the total aboveground biomass or carbon stock, x is the independent variable, b_0 and b_1 are the scaling coefficient and scaling exponent, respectively.

Tree Crown Detection and Delineation

In this study, the region growing segmentation algorithm in eCognition software as an object-based classification program was used for individual tree crown delineation and accurate carbon stock mapping purposes. The region-growing algorithm assumes that the center of tree crown is brighter than the edge of the crown (Culvenor, 2002), then, the treetops are identified as maxima and the shadows between trees as the minimum. The segments are "grown" from these maxima and the valleys act as boundaries. The first step of the region growing is creating the small size, homogeneous objects through the

[DOR: 20.1001.1.16807073.2021.23.1.6.9]

so-called chessboard segmentations from which the brightest pixels are identified as seed pixels (treetops). Radiometric profile of tree crowns was drawn and thresholds determined for local maxima. After chessboard segmentation, a radiometric maximum was identified within each of the individual trees. Different kernel sizes (3, 5, 7 and 9) were designed and evaluated for local maxima algorithm. Finally, radiometric maxima were identified using NDVI and Near-Infrared (NIR) bands and served as the starting points for region growing segmentation. A region-growing process was constrained by two spectral thresholds based on the difference in NDVI and NIR between the original seed and the adjacent candidate pixels, a sharp decrease in NDVI and NIR values showed the crown boundary. The NDVI is insensitive to within-crown brightness variation and, therefore, suitable for detecting true crown edges while minimizing over-segmentation (Blaschke, 2010). This process was iterated until each object was contained by a potential singletree crown. The morphological watershed transformation (Dougherty, 1993) was applied to split the connected and overlapped tree crowns for cluster and conflicted crown separation, and delineation.

Tree Crown Delineation Assessment

The assessment focuses on two aspects of accuracy, including tree detection accuracy and crown delineation accuracy on the images and indices. To evaluate the tree detection rate, we calculate the precision, recall, and overall accuracy measures of the wild pistachio tree detections through comparison with the reference. The precision is the likelihood that a detected wild pistachio tree is valid, as described in Equation (3). The recall is the probability that a wild pistachio tree in reference is detected, as described in Equation (4). The overall accuracy is the average of precision and recall, as described in Equation (5).

$$\text{Precision} = \frac{\text{The number of correctly detected wild pistachio trees}}{\text{The number of all detected objects}} \quad (3)$$

$$\text{Recall} = \frac{\text{The number of correctly detected wild pistachio trees}}{\text{The number of wild pistachio trees in ground truth}} \quad (4)$$

$$\text{Overall Accuracy} = \frac{\text{Precision} + \text{Recall}}{2} \quad (5)$$

For accuracy assessment of tree crowns delineations, we adopted the accuracy indicators that tell the quality of the boundary extent of detected objects, namely, under- and over identification area errors (Ardila *et al.,* 2012). As shown in Figure 3, the delineation accuracy indicators are quantifying how well the extent of an identified object Oi fits a reference object Rj at over and under-identification as Equations (6) and (7):

$$\text{OverID}(O_i) = 1 - \frac{\text{area}(O_i \cap R_j)}{\text{area}(O_i)} \quad (6)$$

$$\text{UuderID}(O_i) = 1 - \frac{\text{area}(O_i \cap R_j)}{\text{area}(R_j)} \quad (7)$$

Where, values of OverID (O_i) and UnderID (O_i) close to zero represent a good match between classified and reference objects and values close to 1 represent a large difference in extent between classification and reference.

The total delineation error indicator in [0, 1] using Equation (8):

$$\text{total error}(O_i) = \sqrt{\frac{\text{OverID}(O_i)^2 + \text{UnderID}(O_i)^2}{2}} \quad (8)$$

2.6. Biomass and Carbon Stock Estimation

The biomass and carbon stock of trees were estimated by using the developed allometric equations and the delineated tree crowns from the satellite image. The estimated biomass and measured (observed) biomass were compared using a paired t-test analysis. Finally, the biomass and carbon stock were estimated for all delineated trees in the study area.

RESULTS

Data Analysis

Descriptive statistics of biophysical features of sample trees are presented in

[DOR: 20.1001.1.16807073.2021.23.1.6.9]

Table 1. The means and ranges of sample trees show that a wide range of trees with different biophysical features was used for modeling.

Biomass and Carbon Stock Allometric Equations

To predict biomass and carbon stock, allometric models were developed using DBH, tree height and crown area as predictors. The allometric equations could fit the data, and more than 80% of observed variation in biomass and carbon stock could be explained by tree crown area. The calculated power model and their results are presented in Table 2.

Tree Crown Detection and Delineation Assessment

Because of solar illumination and different reflectance of trees, a local NIR peak is normally found near the top of a tree crown (Figure 4) which is used to detect local maxima algorithm. The result of tree detection using this algorithm are presented in Table 3, the highest rate of overall accuracy belongs to kernel size of 7. Figures 5, 6 and 7 show the results and steps of tree crown detection and delineation.

The linear regression (Figure 8) exposed a strong relationship with the significant level of α= 0.05 (R^2= 0.95) between the crown area gathered from field surveys and detected by GEOBIA algorithm with a relatively suitable approval of root Means Square error percent (RMSE%) of 14.67% (Table 4). However, this rate was different for different tree crown classes (Table 4). The results showed that more than 88% of delineated crowns had been matched with reference. The total error in small crowns was higher than large crowns and the lowest RMSE (%)= 10.43% and Bias (%)= -0.24% belonged to large crowns.

Biomass and Carbon Stock Estimation

Based on the results, the number of detected wild pistachio tree counted equal to 18301 in the reserved forest of the study area (25 km^2). The average number of trees per hectare was counted about 7.3 in the study area. Based on extracted crowns, the tree level biomass and carbon stock were computed and were calculated in the

Table 1. Descriptive statistics of biophysical attributes of sample trees.

Tree attribute	Mean	Std. D	Max	Min
DBH (cm)	40.8	12.7	79	8
Height (m)	4.5	1.0	7.3	2.1
Crown area (m^2)	30.7	16.1	89.3	2.5
Biomass (kg)	292.9	207.3	961.5	24.2
Carbon stock (kg)	140.0	99.3	460.2	11.5

Table 2. Validation results of allometric equations for wild pistachio biomass and carbon stock.

Variables	Predictors	R^2	F	Sig	Std Error	Equation
Biomass	DBH	0.92	329.7	***	0.24	$Y = 0.053x^{2.283}$
	Height	0.84	145.5	***	0.34	$Y = 2.175x^{3.122}$
	Crown area	0.80	110.0	***	0.38	$Y = 11.028x^{1.007}$
Carbon stock	DBH	0.92	331.4	***	0.24	$Y = 0.025x^{2.289}$
	Height	0.84	145.6	***	0.34	$Y = 1.027x^{3.130}$
	Crown area	0.80	110.3	***	0.39	$Y = 5.225x^{1.010}$

[DOR: 20.1001.1.16807073.2021.23.1.6.9]

Table 3. Tree crown detection evaluation results of applying the local maxima filter algorithm using different kernel size.

Evaluation index	Kernel size			
	3	5	7	9
The number of correctly detected trees	465	483	483	463
The number of all detected objects	582	535	517	508
The number of trees in reference	489	489	489	489
Precision (%)	95.1	98.8	98.8	94.7
Recall (%)	79.9	90.3	93.4	91.1
Overall accuracy (%)	87.5	94.5	96.1	92.9

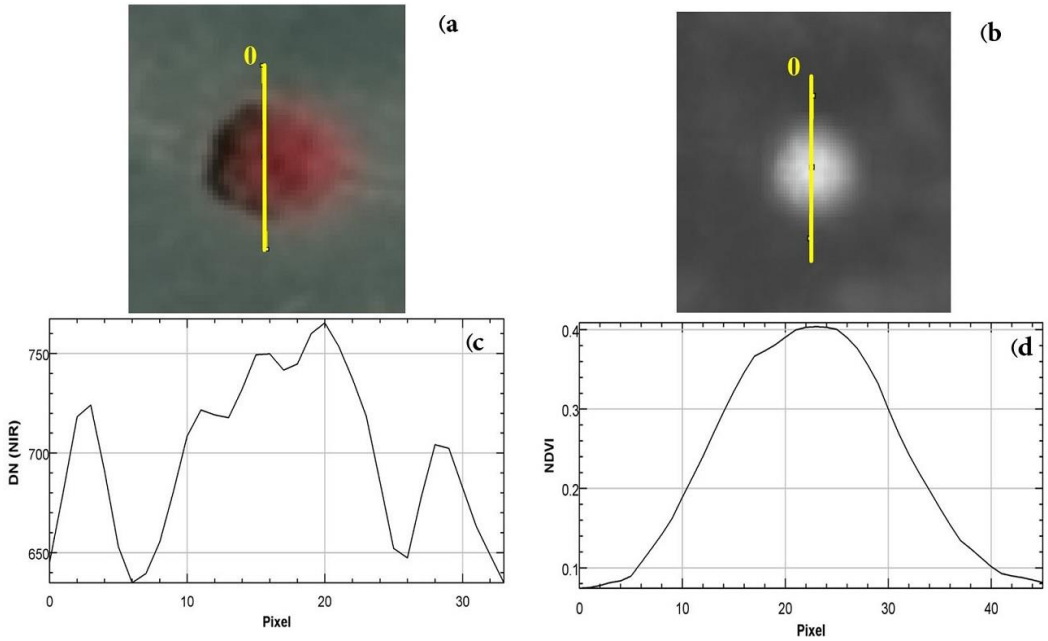

Figure 4. Tree crown is shown on the false colour composite [RGB (432)] with it's near infrared radiometric profile (c) measured along the yellow line (a). The NDVI image of a tree crown (b) with its radiometric profile measured along the yellow line (d).

reserved area (Table 7). The result of the paired t-test showed that there was no significant difference between the estimated biomasses and measured biomasses (Table 6). In addition, the relative RMSE was obtained about 23.6% (Table 5). However, the trees with a small crown class less than 25 m^2 had the highest RMSE compared with other tree crown classes. This means the crown area allometric equation could not accurately estimate the biomass and carbon stock of the trees with small crowns. Figure 9 shows the biomass distribution map of the study area.

DISCUSSION

The methods proposed in this work represent a special approach for individual tree detection in woodland areas that relies only on the availability of VHR imagery. This is useful since satellite imagery provides continuous and systematic coverage over large areas. Images captured by airborne platforms are also an alternative

[DOR: 20.1001.1.16807073.2021.23.1.6.9]

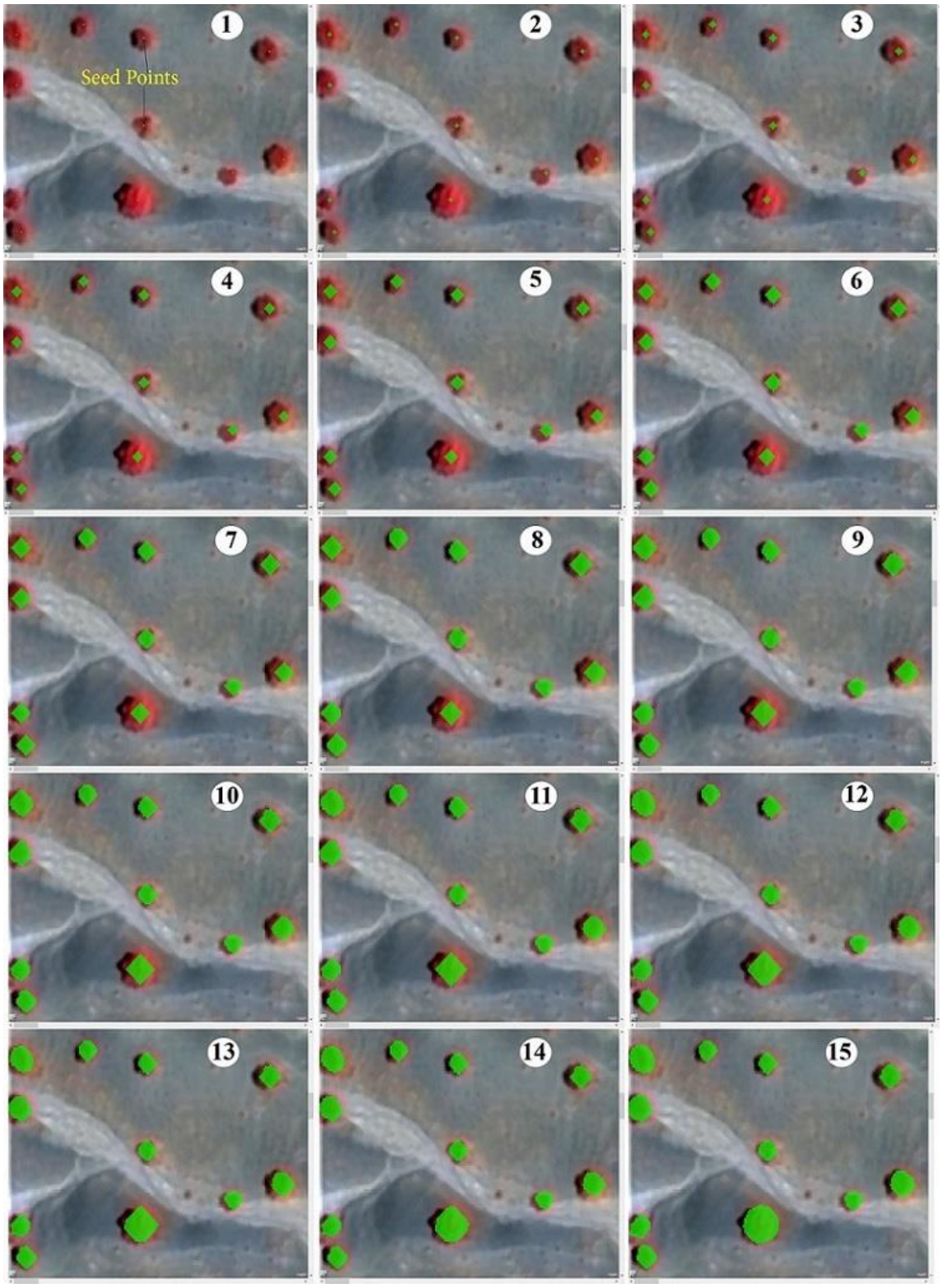

Figure 5. The seed points resulting from running the local maxima filter is shown on Picture 1, and Pictures 2 to 15 show the steps of a region growing algorithm for complete tree crown delineation.

[DOR: 20.1001.1.16807073.2021.23.1.6.9]

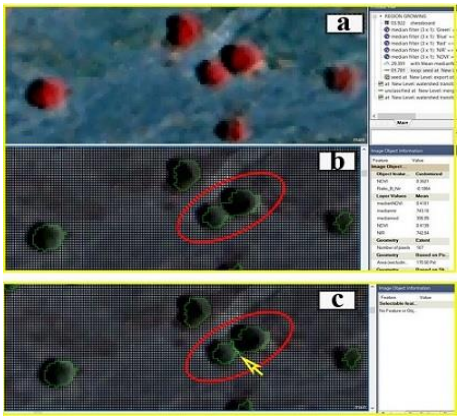

Figure 6. (a) A small window of the false colour composite image [RGB (432)], (b) Delineated crowns after applying the region growing algorithm, and (c) Splitting the cluster connecting crowns using a watershed transformation approach .

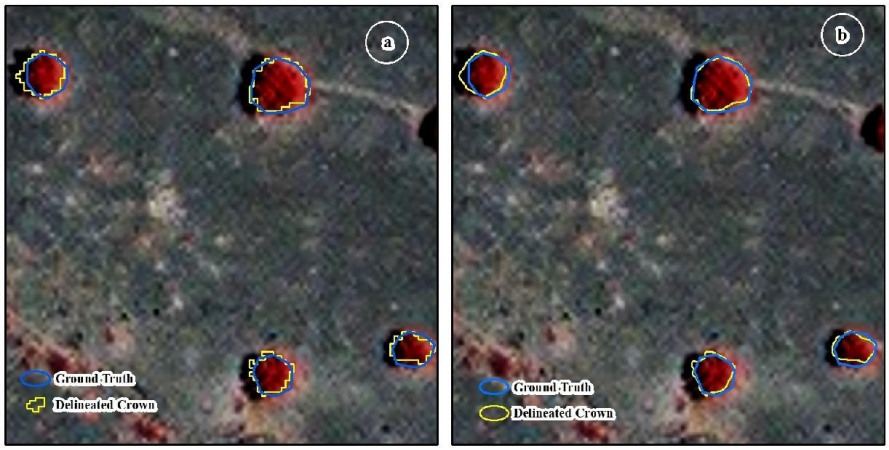

Figure 7. (a) Tree crowns detected by the region growing algorithm (yellow) compared with the reference (blue), and (b) Delineated crowns after refinement and smoothing.

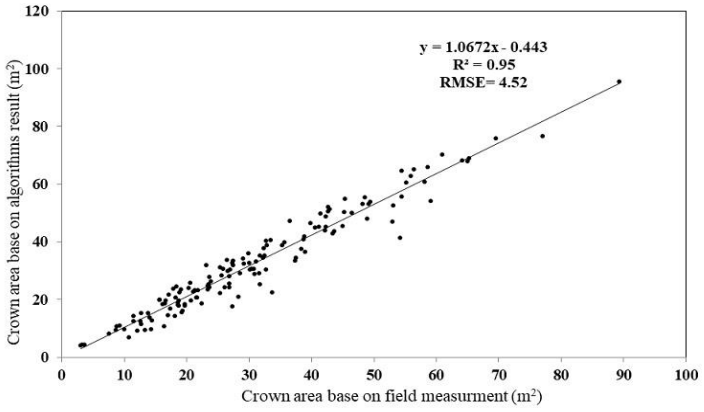

Figure 8. The correlation analysis between detected crown area by algorithm and field surveyed crowns in the sample trees.

[DOR: 20.1001.1.16807073.2021.23.1.6.9]

Table 4. Tree crown delineation errors in different crown size

Crown area class size (m^2)	Under ID	Over ID	Total error	RMSE (%)	RMSE (m^2)	Bias (%)	Bias (m^2)
Small (< 25)	0.11	0.14	0.14	18.02	2.99	-3.71	-0.61
Medium (25-50)	0.07	0.12	0.11	14.24	5.00	-6.39	-2.25
Large (> 50)	0.06	0.10	0.09	10.43	6.40	-0.24	-0.15
All	0.09	0.12	0.12	14.67	4.52	-5.28	-1.63

Table 5. Bias, Bias%, RMSE and RMSE% of the estimated biomass using delineated tree crown.

Allometric equatio	Tree crown class	RMSE (%)	RMSE (Kg)	Bias (%)	Bias (Kg
$Y= 11.028x^{1.007}$	Small (< 25)	44.3	53.2	3.1	3.7
	Medium (25-50)	15.1	45.9	1.9	5.8
	Large (> 50)	25.8	102.8	23.1	92.1
	All	23.6	56.7	7.6	18.2

Table 6. Paired t-test result of measured and estimated biomass comparison.

	Mean	Std. Deviation	Std. Error Mean	Mean difference	t	Sig.
Measured biomass	292.9	207.4	37.8	-5.6	-0.246	0.807
Estimated biomass	299.3	169.0	30.8			

Table 7. The estimated biomass and carbon stock in the reserved area and per hectare using satellite imagery.

Variable	Per hectare (Mg h^{-1})	Reserved Forest (Mg)
Biomass	1.49	3725.0
Carbon stock	0.71	1775.0

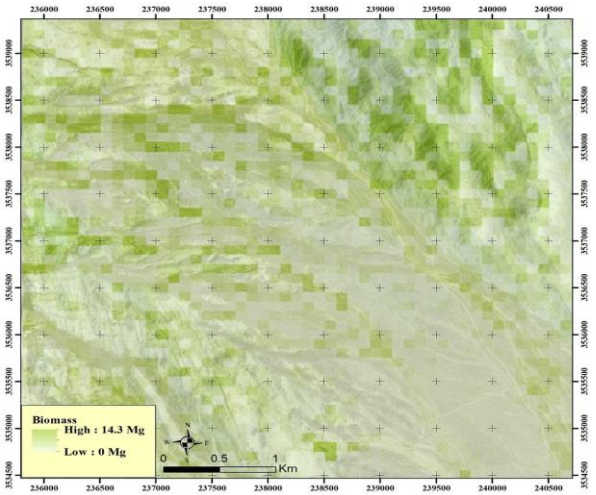

Figure 9. Biomass estimated map of the study area

[DOR: 20.1001.1.16807073.2021.23.1.6.9]

as the input data set for tree detection, as they can provide a higher spatial resolution (for example < 0.5 m) allowing small tree detection. Our result pointed out the application of a segmentation technique (region growing and watershed transformation) was effective in distinguishing tree crowns. The results in crown area detection and delineation showing a higher detection rate (more than 96%) in comparison with similar studies that have been applied for tree crown detection using local maxima. For instance, Karlson *et al* (2014) reported a detection rate of 85.4% in woodland of West Africa using Worldview-2 images, Ardila *et al.* (2012) reported a detection rate between 70–80% using Quickbird imagery to map urban tree cover in the Netherlands, and Bunting and Lucas (2006) reported a detection rate of 71% using Compact Airborne Spectrographic Imager (CASI) imagery in Australian woodlands. Leckie *et al.* (2005) achieved a detection rate between 50–60% of an old growth conifer area in Canada. Higher accuracies have been reported in less complex tree cover conditions, for example, by Pouliot *et al.* (2002), who achieved a detection rate of 91% for a spruce plantation using a modified local maxima approach and multispectral aerial imagery. In addition, Li *et al.* (2017) studied the oil palm tree detection and achieved a detection rate of more than 96% of the oil palm trees, which is similar to our results. The isolated individual trees and low-density of trees in our study area as well as using very high-resolution GeoEye fused images were the important reasons for getting a high detection rate in this study compared with other studies with more complex and dense regions. The relative error in overall delineation accuracy in this study was 14.7%. The results of this study were better compared with previous researches, such as Ardila *et al.* (2012). They reported a relative error of 17-30% compared with a manually delineated reference dataset. Delineation errors as 17.9% have been achieved in even-aged and well-spaced plantation forests (Pouliot *et al.,* 2002). Panagiotidis *et al.* (2017) got a range of 14.3-18.6% for tree crown diameter estimation. However, lower delineation accuracies are to be expected where the tree cover is characterized by high variation in tree crown size distribution (Leckie *et al.,* 2005) and tree species diversity (Ke and Quackenbush 2011). In the study area, despite of varying crown area sizes, the crown of pure stand of wild pistachio trees could be separated better and fewer cluster trees decreased the delineation error. Since there were no allometric equations available for the study area, we developed the local allometric equations. The results showed that the biomass of individual trees can be accurately estimated using allometric equations based on the DBH and the height and crown of the trees (Sohrabi and Shirvani 2012; Chave *et al.,* 2005; He *et al.,* 2013; Lu, 2006).

CONCLUSIONS

The object-based image classification techniques available in commercial software are facilitated practicable and more reliable methods for estimating forest crown in fragmented and degraded dry forest ecosystems. In conclusion, the canopy delineation algorithm used in this study revealed a robust method could produce good estimations of biomass and carbon stock at the individual tree and regional scale level. The relationship between the crown area and carbon stock can be explained by power regression models. The optical images collected from satellite images can be directly used to collect the tree crown area, and indirectly for tree height and or diameter. Allometric relationships between ground-based measurements of tree carbon stock and its crown area with or without tree height can be applied to estimate forest carbon stocks with high certainty. These data are collected over small areas (several hundred of ha) but could be used for inaccessible areas or in sampling design. However, satellite-based estimates of forest biomass and carbon stock will likely be more accessible over the next decade as new technologies emerge and technical capacities are strengthened. Collecting more ground-based data using a proper sampling method, which considers forest type and structure conditions, will be

[DOR: 20.1001.1.16807073.2021.23.1.6.9]

necessary for improving biomass and carbon stock estimations in arid and semi-arid forests.

ACKNOWLEDGEMENTS

This study was made possible by funding of the Gorgan University of Agricultural Science and Natural Resources. The authors would also like to thank experts of Natural Resources and Watershed Management Administration of South Khorasan Province for their supports and cooprations in the field measurements.

REFERENCES

1. Ardila, J. P., Bijker, W., Tolpekin, V. A. and Stein, A. 2012. Context-Sensitive Extraction of Tree Crown Objects in Urban Areas Using VHR Satellite Images. *Int. J. App. E. Observ. Geoinfo*., **15:** 57-69.
2. Benediktsson, J. A., Pesaresi, M. and Amason, K. 2003. Classification and Feature Extraction for Remote Sensing Images from Urban Areas Based on Morphological Transformations. *IEEE Tran. Geosc. Rem. Sen.*, **41(9):** 1940-9.
3. Blaschke, T. 2010. Object-Based Image Analysis for Remote Sensing. *ISPRS J. Photo. Rem. Sen.*, **65(1):** 2-16.
4. Brandtberg, T. and Walter, F. 1998. Automated Delineation of Individual Tree Crowns in High Spatial Resolution Aerial Images by Multiple-Scale Analysis. *Mach. Vis. App.*, **11(2):** 64-73.
5. Brown, S. 1997. Estimating Biomass and Biomass Change of Tropical Forests a Primer. FAO Forestry Paper: 134, FAO, Food and Agriculture Organization of the United Nations, Rome.
6. Brown, S. 2002. Measuring Carbon in Forests: Current Status and Future Challenges. *En. Pol.*, **116(3):** 363-72.
7. Bunting, P. and Lucas, R. 2006. The Delineation of Tree Crowns in Australian Mixed Species Forests Using Hyperspectral Compact Airborne Spectrographic Imager (CASI) Data. *Rem. Sen En.*, **101(2):** 230-48.
8. Cairns, M. A., Brown, S., Helmer, E. H. and Baumgardner, G. A. 1997. Root Biomass Allocation in the World's Upland Forests. *Oecologia*, **111:** 1–11.
9. Chave, J. C., Andalo, S., Brown, M. A., Cairns, J. Q., Chambers, D. and Folster, H. 2005. Tree Allometry and Improved Estimation of Carbon Stocks and Balance in Tropical Forests. *Oecologia*, **145:** 87 - 99.
10. Chavez, J. R., Pat, S., Sides, C. and Anderson, J. A. 1991. Comparison of Three Different Methods to Merge Multiresolution and Multispectral Data: Landsat TM and SPOT Panchromatic. *Phot. Eng. Rem. Sen.*, **57(3):** 265-303
11. Culvenor D. S. 2002. TIDA: An Algorithm for the Delineation of Tree Crowns in High Spatial Resolution Remotely Sensed Imagery. *Com. Geosci.*, **28(1):** 33-44.
12. Definiens. 2006. *Definiens Professional 5 Reference Book.* Definiens AG, Germany, 471 PP.
13. Dougherty, E. R. 1993. Mathematical Morphology in Image Processing. "Optical Engineering". CRC Press, New York.
14. Drake, J. B., Dubayah, R. O., Clark, D. B., Knox, R. G., Blair, J. B., Hofton, M. A., Chazdon, R. L., Weishampel, J. F. and Prince, S. 2002. Estimation of Tropical Forest Structural Characteristics Using Large-Footprint Lidar. *Rem. Sen. En.*, **79(2):** 305-19.
15. Drake, J. B., Knox, R. G., Dubayah, R. O., Clark, D. B., Condit, R., Blair, J. B. and Hofton, M. 2003. Above-Ground Biomass Estimation in Closed Canopy Neotropical Forests Using Lidar Remote Sensing: Factors Affecting the Generality of Relationships. *Glob. Eco. Biogeo*., **12(2):** 147-59.
16. Eckert, S. 2012. Improved Forest Biomass and Carbon Estimations Using Texture Measures from World View-2 Satellite Data. *Rem. Sen.*, **4:** 810–829.
17. Erikson, M., Olofsson, K., 2005. Comparison of Three Individual Tree Crown Detection Methods. *Mach. Vision Applic.* **16**: 258–265.
18. Evans, C., Jones, R., Svalbe, I. and Berman, M. 2002. Segmenting Multispectral Landsat TM Images into Field Units. *IEEE Tran. Geosc. Rem. Sen.*, **40(5):** 1054-64.
19. FAO. 2004. Carbon Sequestration in Dryland Soils. In: "*World Soil Resources Reports"*. FAO Publishing Management Service, Rome, Italy. 129 p.
20. Feldpausch, T. R., Banin, L., Phillips, O. L.; Baker, T. R.; Lewis, S. L., Quesada, C. A. and Affum Baffoe, K. 2011. Height-Diameter Allometry of Tropical Forest Trees. *Biogeoscience*, **8(5):** 1081-106.
21. Gibbs, H. K., Brown, S., Niles, J. O. and Foley, J. A. 2007. Monitoring and Estimating

[DOR: 20.1001.1.16807073.2021.23.1.6.9]

Tropical Forest Carbon Stocks: Making REDD a Reality. *Envi. Res. Let.*, **2:** 1-13.
22. Goetz, S. J., Baccini, A., Laporte, N. T., Johns, T., Walker, W., Kellndorfer, J. and Sun, M. 2009. Mapping and Monitoring Carbon Stocks with Satellite Observations: A Comparison of Methods. *Carb. Bal. Man.*, **4(1):** 2.
23. Hay, G. J. and Castilla, G. 2008. Geographic Object-Based Image Analysis (GEOBIA): A New Name for a New Discipline. In "*Object-Based Image Analysis: Spatial Concepts for Knowledge-Driven Remote Sensing Applications*", (Eds.): Blaschke, T., Lang, S. and Hay, G. J. *Springer Berlin Heidelberg*, Heidelberg, Berlin, PP. 75-89.
24. He, Q., Chen, E., An, R. and Li, Y. 2013. Aboveground Biomass and Biomass Components Estimation Using LiDAR Data in a Coniferous Forest. *Forests*, **4(4):** 984-1002.
25. Helmut, M. 2008. Object Extraction in Photogrammetric Computer Vision. *ISPRS J. Photo. Rem. Sen.*, 63(2): 213-222.
26. Huang, X. and Zhang, L. 2008. An Adaptive Mean-Shift Analysis Approach for Object Extraction and Classification from Urban Hyperspectral Imagery. *IEEE Tran. Geosc. Rem. Sen.*, **46(12):** 4173– 4185.
27. Hussin, Y. A., Gilani, H., Van Leeuwen, L., Murthy, M. S. R., Shah, R., Baral, S., Tsendbazar, N. -E., Shrestha, S., Shah, S. K. and Qamer, F. M. 2014. Evaluation of Object-Based Image Analysis Techniques on Very High-Resolution Satellite Image for Biomass Estimation in a Watershed of Hilly Forest of Nepal. *Appl. Geoma*., **6:** 59–68.
28. Karlson, M., Reese, H. and Ostwald, M. 2014. Tree Crown Mapping in Managed Woodlands (Parklands) of Semi-Arid West Africa Using WorldView-2 Imagery and Geographic Object-Based Image Analysis. *Sensors*, **14(12):** 22643.
29. Ke, Y. and Quackenbush, L. J. 2011. A Review of Methods for Automatic Individual Tree-Crown Detection and Delineation from Passive Remote Sensing. *Int. J. Rem. Sens.*, **32(17):** 4725-47.
30. Ke, Y. and Quackenbush, L. J. 2007. Forest Species Classification and Tree Crown Delineation Using QuickBird Imagery. *ASPRS 2007 Annual Conference Tampa*, May 7-11, 2007, Florida,
31. Kuyah, Sh., Muthuri, C., Jamnadass, R., Mwangi, P., Neufeldt, H. and Dietz, J. 2012. Crown area Allometries for Estimation of Aboveground Tree Biomass in Agricultural Landscapes of Western Kenya. *Agro. Sys.*, **86(2):** 267-77.
32. Lal, R. 2004. Carbon Sequestration in Dry Land Ecosystems. *Env. Man.*, **33(4):** 528-44.
33. Leckie, D. G., Gougeon, F. A., Walsworth, N. and Paradine, D. 2003. Stand Delineation and Composition Estimation Using Semi-Automated Individual Tree Crown Analysis. *Rem. Sen. En.*, **85(3):** 355-69.
34. Leckie, D. G., Gougeon, F. A., Tinis, S., Nelson, T., Burnett, C. N. and Paradine D. 2005. Automated Tree Recognition in Old Growth Conifer Stands with High Resolution Digital Imagery. *Rem. Sen. En.*, **94(3):** 311-26.
35. Li, W., Fu, H., Yu, L. and Cracknell, A. 2017. Deep Learning Based Oil Palm Tree Detection and Counting for High-Resolution Remote Sensing Images. *Rem. Sen.*, **9(1):** 22.
36. Li, C., Li, Y. and Li, M. 2019. Improving Forest Aboveground Biomass (AGB) Estimation by Incorporating Crown Density and Using Landsat 8 OLI Images of a Subtropical Forest in Western Hunan in Central China. *Forests*, **10:** 104.
37. Lu, D., 2006. The Potential and Challenge of Remote Sensing-Based Biomass Estimation. *Int. J. Rem. Sens.*, **27(7):** 1297-328.
38. Mayer, H., 2008. Object Extraction in Photogrammetric Computer Vision. ISPRS J. Photogrammetry and Remote Sensing, **63(2)**: 213-222.
39. Mora, B., Wulder, M. A. and White J. C. 2010. Segment-Constrained Regression Tree Estimation of Forest Stand Height from Very High Spatial Resolution Panchromatic Imagery over a Boreal Environment. *Rem. Sen. En.*, **114(11):** 2474-2484.
40. Mousavi, B. 2015. Comparison of High Resolution (Quickbird) and Medium Resolution (Landsat8-OLI) Satellite Images Capability in the Estimation of Trees Aboveground Biomass. A Thesis of Master Student in Forest Science, Gorgan University of Agriculture and Natural Resources, 132 PP.
41. Mukono, D. and Sambaiga, R. 2016. A Critical Review on the Major Conceptual Strands/debates on the Reduced Emission from Deforestation and Forest Degradation (REDD+) and Improved Social Livelihoods. *Environ. Manage. Sust. Dev.*, **5:** 140.
42. Myint, S. W., Gober, P., Brazel, A., Grossman-Clarke, S. and Weng, Q. 2011. Per-Pixel vs. Object-Based Classification of Urban Land Cover Extraction Using High Spatial

[DOR: 20.1001.1.16807073.2021.23.1.6.9]

Resolution Imagery. *Rem. Sen. En.*, **115(5):** 1145-61.
43. Panagiotidis, D., Abdollahnejad, A., Surový, P. and Chiteculo, V. 2017. Determining Tree Height and Crown Diameter from High-Resolution UAV Imagery. *Int. J. Rem. Sens.*, **38(8-10):** 2392-410.
44. Platt, R. V. and Schoennagel, T. 2009. An Object-Oriented Approach to Assessing Changes in Tree Cover in the Colorado Front Range 1938–1999. *For. Ecol. Man.*, **258(7):** 1342-9.
45. Pouliot, D. A., King, D. J., Bell, F. W. and Pitt, D. G. 2002. Automated Tree Crown Detection and Delineation in High-Resolution Digital Camera Imagery of Coniferous Forest Regeneration. *Rem. Sen. En.*, **82(2–3):** 322-34.
46. Pu, R. and Landry, Sh. 2012. A Comparative Analysis of High Spatial Resolution IKONOS and WorldView-2 Imagery for Mapping Urban Tree Species. *Rem. Sen. En.*, **124:** 516-33.
47. Saliola, A. 2014. Object-Based Image Analysis for the Delineation of Canopy Gaps and Individual Tree Crowns Using Multi-Source Data: A Case Study in Halliburton Forest, Ontario. MSc. Thesis, University of Toronto.
48. Sohrabi, H. and Shirvani, A. 2012. Allometric Equations for Estimating Standing Biomass of Atlantic Pistache (*Pistachia atlantica* var. Mutica) in Khojir National Park. *Iran. J. For.*, **4(1):** 55-64. (Persian)
49. Velarde, S. J., Barona, E., Capella, J. L., Castro, A., Hyman, G., Maran, J. A., Sandoval, M., Tito, M. R. and Ugarte-Guerra, L. J. 2010. *Reducción de Emisiones de Todos los Usos del Suelo: Reporte del Proyecto REALU Perœ Fase 1*. ICRAF Working Paper.
50. Wu, C., Shen, H., Wang, K., Shen, A., Deng, J. and Gan, M. 2016. Landsat Imagery-Based Above Ground Biomass Estimation and Change Investigation Related to Human Activities. *Sustainability*, **8:** 159.
51. Wulder, M. A., White, J. C., Fournier, R., Luther, J. E. and Magnussen, S. 2008. Spatially Explicit Large Area Biomass Estimation: Three Approaches Using Forest Inventory and Remotely Sensed Imagery in a GIS. *Sensors* (Basel), **8(1):** 529-560.
52. Zaki, N. A. M., Abd Latif, Z., Zainal, M. Z. and Zainuddin, K. 2015. Individual Tree Crown (ITC) Delineation Using Watershed Transformation Algorithm for Tropical Lowland Dipterocarp. *International Conference on Space Science and Communication (Iconspace 2015)*, Langkawi , Malaysia, PP. 237-242.

برآورد میزان زی‌توده و ذخیره کربن گونه بنه در نواحی خشک با استفاده از تصاویر ماهواره ای GeoEye-1

ر. باقری، ش. شتایی جویباری، و ی. عرفانی فرد

چکیده

برآورد دقیق مکانی زی‌تودهٔ روی زمین در مناطق وسیع مورد نیاز برنامه‌ریزان منابع طبیعی می‌باشد. این تحقیق به‌منظور ارزیابی زی‌توده و ذخیره کربن درختان بنه بر اساس تشخیص و شناسایی محدوده تاج درختان با استفاده از تصاویر ماهواره GeoEye-1 و روابط آلومتریک در ذخیره‌گاه جنگلی این گونه در شهرستان نهبندان استان خراسان جنوبی در شرق ایران انجام شد. زی‌توده درختان نمونه با استفاده از نمونه برداری میدانی و روش‌های تجربی تعیین شد. به‌علاوه زی‌توده تنه درختان با استفاده از حجم و چگالی چوب تعیین شد. معادلات آلومتریک زی‌توده و ذخیره کربن بر اساس سطح تاج، قطر برابر سینه و ارتفاع درختان تهیه شد. تاج درختان بر روی تصویر ماهواره‌ای با استفاده از الگوریتم‌های حداکثر محلی و رشد نواحی شناسایی

[DOR: 20.1001.1.16807073.2021.23.1.6.9]

گردید. همچنین روش قطعه‌بندی حوضه برای جداسازی تاج‌های به‌هم‌پیوسته استفاده شد. الگوریتم‌های اجرا شده با استفاده از تاج درختان برداشت زمینی ارزیابی گردید. نتایج نشان داد معادله آلومتریک بر اساس سطح تاج بیش از ۸۰ درصد تغییرات زی‌توده و ذخیره کربن را تبیین می‌کند. به‌علاوه روش تشخیص و تعیین محدوده تاج درختان قابل قبول بود. به‌طورکلی نتایج نشان داد روش مورداستفاده و ترکیب معادلات آلومتریک با استخراج تاج درختان بنه بر اساس تصاویر ماهواره‌ای با قدرت تفکیک مکانی بالا امکان تهیه نقشه دقیق زی‌توده و ذخیره کربن درختان بنه را در مناطق خشک و نیمه‌خشک فراهم می‌نماید.

[DOR: 20.1001.1.16807073.2021.23.1.6.9]